LOW SPEED VS HIGH SPEED TESTING OF LP TURBINE BLADE-WAKE INTERACTION

M.Vera
Whittle Laboratory
University of Cambridge
U.K.

H.P.Hodson
Whittle Laboratory
University of Cambridge
U.K.

ABSTRACT

The techniques employed in high speed linear cascade testing to simulate the effect of unsteadiness are presented and compared with low speed counterparts. Results are obtained from a high speed cascade and a low speed cascade. Both are models of an existing (conventional) low pressure turbine blade. They are compared under steady and unsteady flow conditions. The results show that the same quantitative values of losses are obtained, proving the validity of the low speed approach for profiles with an exit Mach number of the order of 0.64. The range of validity of the conclusions is extended by reference to a profile designed using current low pressure turbine design practice.

INTRODUCTION

The development of the low pressure turbine (LPT) has reached a stage where rises in efficiency are difficult to obtain. Due to the large aspect ratios of LPT stages, their contribution to the total weight of the engine could represent one third of the total weight. Therefore, one of the current trends that designers have adopted is to improve the overall performance of the LPT by reducing its weight. This new philosophy leads to fewer blades each of which carries a greater aerodynamic load.

The LPT operates at the lowest Reynolds number in the whole engine. This means that the development of the boundary layers will be determined by the transition from laminar to turbulent flow. Increasing the aerodynamic load increases the diffusion on the rear part of the blade and thus the risk of separation. The resulting blade usually features a large separation bubble in steady flow conditions. This can be partially or totally suppressed by transition caused by the wakes coming from an upstream row of blades. Due to the ability of the wakes shed by an upstream row to promote transition in the neighborhood of separation, the study of wake-boundary interactions is of primary interest in the LPT environment. The large aspect ratio of the LPT blades (typically between 3 and 7) makes them appropriate for linear cascade testing.

Previous studies on wake induced transition phenomena for high speed flows have been carried out by others researchers (Brunner et. al, 2000 and Coton et. al, 2002) but still, very little is known about the topic. This fact together with the current limitations of the CFD tools suggests that experimental studies of blade-wake interaction phenomena in high speed flows are needed. Even though the experimental techniques used in high speed testing are conceptually the same as those used in low speed, the problems encountered tend to be magnified at high speed. In addition, new challenges arise. Therefore, we should question when it is worth doing high speed cascade testing. This paper aims to answer this question. It examines the extent to which the results from the low speed approach are meaningful.

This paper follows previous comparisons between high speed and low speed testing, (Wisler, 1984), (Hodson and Dominy, 1993), by presenting a comparison between high speed and low speed testing of LPT linear cascades. In the main part of this paper, two profiles are compared. These profiles are not identical but they both are intended to model an existing LPT blade in the cascade environment at low speed or at high speed. Facilities and instrumentation will also be compared. Finally, results from a modern LPT blade will be presented to demonstrate the extent to which the conclusions are valid.

NOMENCLATURE

C	Chord
C_d	Drag coefficient
D	Drag force
d	Bar diameter
F	Reduced frequency
f	Bar passing frequency
KSI	Energy loss coefficient $= \frac{T_{s3} - T_{ise,3}}{T_{01} - T_{s3}}$
m	Mass
Ma	Mach number

P	Pressure
PS	Pressure surface
R	Radius
Re	Reynolds number
s	Pitch
SS	Suction surface
T	Temperature
U	Speed of the bars
V	Absolute velocity
W	Relative velocity
Y_p	Stagnation pressure loss coefficient = $\frac{P_{01} - P_{03}}{P_{01} - P_{s3}}$
α	Absolute flow angle
β	Relative flow angle
d	Deflection
ϕ	Flow coefficient
O	Rotational speed

Subscripts

0	Stagnation. Upstream the bars row
1	Downstream the bars row
2	Downstream the cascade
3	Mixed-out conditions
bar	Related to the bars
design	Related to the design conditions
is	Isentropic
s	Static
x	Axial
8	Related to the freestream

DESIGN PROCESS

Design of the blade profile.

In this paper, the description of the design procedure starts from the point where the section of the LPT to be modelled is already known, i.e., all the geometric and aerodynamic parameters of the corresponding section are given. The modelling of a section aims to obtain a blade with the same shape of Mach number distribution as the one around the blade in the turbine.

In high speed linear cascade modelling, it is common to set the exit angle of the blade to be the same as the one in the turbomachine. The design exit Reynolds and exit Mach numbers are also chosen to be the same as in the engine.

Linear cascades consist of two endwalls between which the constant section blades are placed. This section should be taken from a stream-surface of the blade row to be modelled. Only in few cases is the stream tube divergence of the turbomachine correctly modelled. In such cases, the endwalls of the cascade are not parallel. Furthermore, if the stream surface is cylindrical then the shape of the blade and the inlet flow angle can be exact copies of those in the turbine. In general, the above are not possible because the endwalls are parallel and the stream surface is not cylindrical (or conical). Under these circumstances, the inlet flow angle is modified slightly in order to achieve the same inlet Mach number as in the turbine. This makes it possible to obtain the same Mach number distribution as the one existing in the engine. This is achieved by redesigning the profile.

A high speed continuous facility requires a high power compression system. Thus, in order to make it affordable, the mean flow rate through the test section tends to be small (Hodson and Dominy, 1993). This constrains the size of the blades. In this context, care must be taken to ensure that the aspect ratio of the blades is large enough to create a substantial region of 2D flow in the test section. An aspect ratio above 2 is needed to ensure this.

To model the blade at low speed, more compromises are required. The aim is again to obtain the same shape of Mach number (velocity) distribution as the one in the turbine. The Reynolds number, the exit angle and the ratio of inlet to exit Mach number (velocity) are usually maintained as close as possible to the corresponding values in the engine. The inlet angle and the shape of the blade must now be modified to account for the effects of compressibility as well as stream tube divergence. The Prandtl-Glauert rule (Hoerner, 1965) and the general absence of stream tube divergence in the cascade are of primary importance when designing a low speed model of a high speed profile (Wisler, 1984). The typical change in the inlet angle is of the order of 5-8 degrees.

Low speed cascades, by virtue of their larger scale and lower speeds, offer several advantages over high speed cascades. In low speed cascades, the maximum size of the blades is determined by the need to keep the lowest Reynolds number the same as in the real machine and by the need to have measurable pressure differences when running at or close to atmospheric pressure at the low velocity the large scale implies.

The above discussion shows that in using high speed cascades, few compromises are needed to achieve a model of the real blade. Indeed, true similarity can be obtained sometimes. In the case of low speed cascades, more compromises are required. Typical sizes of the resulting LPT blades are shown in Table 1.

Choosing the bars

To achieve a realistic simulation of the rotor-stator interaction, several similarity parameters must be correctly matched. The method used to choose the size and the pitch of the bars is the same in low and high speed cascade testing and it is presented below. Only by following this procedure is a good simulation of the rotor-stator interaction situation achieved.

To correctly reproduce the kinematics of the wake-blade interaction, the flow angle β_1 in the bar

relative frame of reference, is matched to that of the upstream bladerow in the LPT. The relative and absolute inlet flow angles and the inlet axial velocity to the cascade, V_{x1}, then give the speed of the bars, U, from the velocity triangles at the inlet of the cascade.

The reduced frequency of the machine not only sets the ratio of the convection time scale to the wake passing time scale, but it also sets the ratio of the viscous diffusion time scale to wake passing time scale. Therefore, it must be matched if a realistic rotor-stator interaction is to be achieved. The reduced frequency, F, and the bar passing frequency, f, are related according to the expression

$$F \equiv f\frac{C}{V_2} = \frac{U}{s_{bar}}\frac{C}{V_2} \propto f\frac{x}{U} \qquad (1)$$

which provides the bar passing frequency and the pitch of the bars, s_{bar}. The reduced frequency is defined in terms of the exit velocity of the cascade. This is because the most important wake-blade interactions tend to occur in the latter half of the blade passage. Typical values of the bar passing frequencies for high speed and low speed cascades are given in Table 1.

Pfeil and Eifler (1976) showed that the structure of the far wake of an airfoil and that of a cylindrical body of the same drag is almost the same. If an estimation of the stagnation pressure losses of the blade row to be simulated is known, the diameter of the bars, d, can be obtained according to

$$Y_p = \frac{dC_d}{s_{bar}Cos\beta_1} \qquad (2)$$

which is exact for low speed flows.

An estimation of the drag coefficient of the bars, C_d, at the relative conditions that Y_p represents, must be known. Typical dimensions of the resulting diameters of the bars are given in Table 1. These values are of the same order than the trailing edge thickness of the upstream blade row.

Once all the previous values are fixed, the ratio between the pitch of the cascade, s, and the pitch of the bars is known. Also, the flow coefficient of the bars, ϕ, is given by

$$\phi = \frac{V_{x1}}{U} \qquad (3)$$

	High speed	Low speed
Chord	50mm	200mm
Bar diameter	0.41mm	2mm
Bar passing frequency	3kHz	200Hz

Table 1 Typical dimensions of blades and bars in low speed and high speed cascades.

TEST FACILITIES AND INSTRUMENTATION

For the present work, two linear cascade facilities have been used. The description of the low speed passing bar linear cascade facility was previously documented by Banieghbal et. al, (1995). It is the aim of this paper to describe the high speed rotating bar linear cascade facility and to compare it with its low speed counterpart.

Transonic cascade facility

The high speed experiments were carried out in the transonic cascade facility at the Whittle laboratory. This is a continuous flow, closed-circuit variable density wind tunnel where Reynolds and Mach number can be fixed independently. Two vacuum pumps, working in parallel, are used to achieve sub-atmospheric pressures. A compressor is used to control the pressure ratio and thus the Mach number of the flow within the circuit. To control the humidity of the air, some of the air is passed through a dryer. The temperature variation can be limited by adjusting the cooling system. Before entering the plenum, the air passes through a honeycomb and screen in order to filter the air and to break up any large scale structures that may exist in the flow. At the exit of the plenum, the flow is accelerated in a convergent nozzle and it is discharged into the large exit plenum that contains the test section.

Wake generators

The presence of the wakes shed from an upstream blade row is simulated using a wake generator. In the low speed cascades, the wake generator consists of bars fitted between two belts placed on either side of the side walls. The wake generator is driven by a motor by means of mechanism of belts and pulleys and provides linear motion to the bars. This is shown in figure 2.

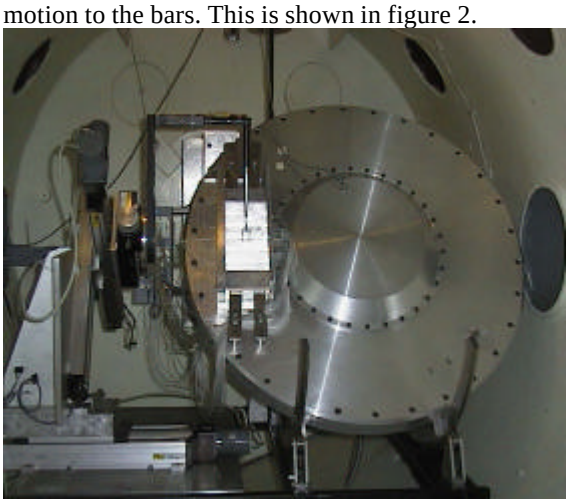

Figure 1. High speed rotating bar rig

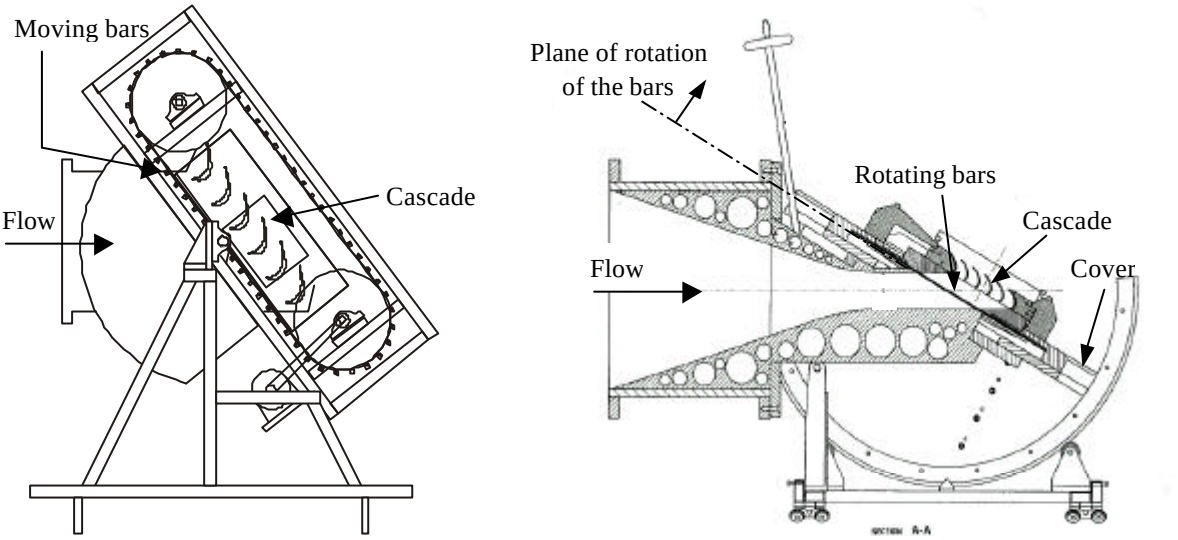

Figure 2. Cross sections of the low speed moving bar rig (left) and the high speed rotating bar rig (right)

In high-speed flows, the matching of similarity parameters demands a higher speed from the bars. For mechanical reasons this cannot be achieved with the type of bar passing wake generator typical of low speed rigs. Instead, the high speed bar wake generator consists of a number of metal bars equally spaced at the outer periphery of a disk that rotates in a plane parallel to the leading edge plane of the cascade. In this way the circumferential speed of the bars can be increased to the levels that are required in the cascade experiments. A cover encloses the rotating disk and bar assembly thus creating a sealed chamber containing the bars. This sealed cavity is needed to prevent the leakage that would occur if the cavity were opened to the plenum, i.e., to exit conditions. Low speed cascade testing tends to suffer from this sort of leakage. The cover has a rectangular opening aligned with the exit of the convergent nozzle over which the cascade is mounted. A similar configuration has successfully been used in Oxford (Doorly, 1984).

In both, low and high speed cascade testing, the wake generator is driven by an electric motor that keeps the rotation at constant speed. Both the low speed bar passing rig and the high speed bar rotating rig were designed to cover a wide range of operating conditions resulting from the independent variation of the geometric and flow parameters involved in the study of the unsteadiness created for the wakes shed by an upstream blade row. In figure 1 a rear view of the high speed bar passing rig is shown. Figure 2 shows the cross sections of the facilities in both low speed and high speed.

Inlet Periodicity

In both high and low speed cascade testing, the cascades consist of blades of constant section mounted on two sidewalls. In the low speed cascade two fake passages are left at the top and at the bottom of the cascade in order to control the periodicity of the cascade. Movable sheets regulate the mass flow rate through these fake passages thus controlling the inlet periodicity. Controlling the inlet periodicity is easier in high speed due to the sealed chamber that contains the bars. Therefore, the fake passages are not used and are replaced by small spanwise bleed slots.

Bars

The bars move across the front of the cascade thus simulating the upstream blade row.

In the low speed moving bar rig, nylon or steel bars are fitted into the belts. When the bars rotate around the pulley, they are subjected to a traverse centrifugal loading. This loading produces a deflection in the bars that constraints their performance. For a given aspect ratio of the cascade, the maximum deflection of the bars, d, due to the transverse centrifugal loading can be shown to be of the form,

$$\frac{\delta}{C} \propto \frac{Re^2}{C^2} \qquad (4)$$

The relation (4) shows that in order to reduce the deflection of the bars, a larger chord is needed for a given Reynolds number.

In the high speed rotating bar rig the bars are made of hypodermic tube. They are fitted at the outer periphery of the rotating disk. When the bars cross the test section, they are subjected to a transverse aerodynamic loading. This loading

deflects the bars and thus limits their performance. The deflection, d, must be smaller than the distance between the bars and the cover[1]. For a given flow coefficient, ϕ, this deflection can be shown to be of the form,

$$\frac{\delta}{C} \propto \Omega^2 \rho_{air} R_{disk}^2 \qquad (5)$$

where R_{disk} is the radius of the rotating disk and O is the rotational speed of the bars. From (5), it is seen that a disk of a small radius could reduce the deflection for a given density of the air and rotational speed of the bars. Having a small disk is compromised by the need to have a substantial region of 2D flow at the inlet of the cascade. Moreover, if the Mach number is also given, the relation (5) can be further simplified to,

$$\frac{\delta}{C} \propto \frac{Re}{C} \qquad (6)$$

From (6), it is seen that in order to reduce the deflection, a larger chord is needed for a given Reynolds number and Mach number.

The bars are also subjected to an axial loading due to centrifugal effects. The axial tension tends to straighten the bars and thus reduces their deflection. The deflection can be reduced, for a given diameter of the bars, by placing a weight on the tip of the bars. Additionally, when the bars leave the test section, the aerodynamic loading ceases. This transient leads to forced vibrations of the bars. By placing the weight on the tip of the bars, these vibrations are also reduced. The maximum mass that can be used is given by the maximum strength of the material.

The above discussion shows how to avoid some the mechanical constraints limiting the performance of the bars. These limitations must be taken into consideration when fixing the scale of the cascade. Only in this way can a realistic simulation of the blade-wake interaction phenomena be achieved.

Instrumentation

The instrumentation for high speed measurements is conceptually the same as that used for low speed testing. This instrumentation is described by Banieghbal et. al, (1995). The differences between the acquisition of data in low speed and high speed flows are due to the different scales of the values to be measured. This influences the quality of the measurements by influencing the resolution of the output of the signal and the resolution of the characteristic time.

The differences between the pressures to be measured in high speed flows are higher than those in low speed flows. Thus, data are easier to measure in high speed flows although a larger full scale range transducer are needed. The sensitivity of the transducers along with the signal to noise ratio, set the minimum pressure difference that can be measured. This fixes the minimum velocity that can be measured for a given density and limits the maximum chord at low Reynolds numbers in low speed flows.

The calibration of hot wires used for incompressible flows relates the rate of convective heat transfer to the velocity (Reynolds number) of the flow. The calibration of hot wires used for compressible flows is more complicated. The heat transfer depends on the Mach number of the flow as well as on the Reynolds number based on the diameter of the wire. Therefore, in using a hot wire in compressible flows a calibration map is required. This map must include variations of Mach number and Reynolds number. These problems do not appear when using hot films probes as pseudo-calibrations are used (Hodson, 1984).

The response frequency of conventional hot films and hot wires is of the order of 25 to 50kHz. The scale of the boundary layers and the freestream velocity indicates that the lowest turbulent frequencies are expected to be of the order of 3kHz and 100kHz for the low speed and high speed blades respectively. For a complete characterization of these lowest turbulent frequencies (phase and amplitude), the acquisition frequency would have to be of the order of 10 times larger. Therefore, the lowest turbulent frequencies can be characterized only for low speed flows. Additionally, Table 1 presents the typical value of the bar passing frequency in high speed cascade testing. This is of the order of 3kHz. Thus, for a given the response frequency of the anemometers, a poorer resolution of the bar passing period is obtained for high speed cascades.

The frequency response of typical fast-response miniature pressure transducers is of the order of 100-500kHz. If the pressure transducers are flush mounted, which is the configuration that gives the best frequency response, the scale of the transducer limits the maximum frequency that can be resolved. This maximum frequency is determined by the speed of the flow divided by the scale of the transducer. In low speed measurements, this value is of the order of 5-10kHz. In high speed measurements, it is of the order of 100kHz. In both cases, the frequency response is well above the respective bar passing frequency. Both higher frequency limits are of the same order of magnitude as the respective lowest turbulent frequencies. This means that the lowest turbulent frequencies can be captured. This is important in high lift LP turbines (Stieger and Hodson, 2003).

[1] This distance is shorter than the axial gap between the bars and the leading edges of the cascade

RESULTS

This section examines the extent to which the low speed results are meaningful. To do so, the results from a high speed and a low speed cascade both being the model of an existing LPT blade are compared for steady and unsteady flow conditions. The comparison includes Mach number (velocity) distributions, profile loss measurements and surface mounted hot-film measurements.

Inlet conditions to the cascade

The time mean conditions at inlet to the cascade are affected by the bars. These effects are due to the creation of entropy by the bars and work done by the component of the drag force of the bars in the direction of movement of the bars.

In the ideal case, the time mean conditions at the inlet of the cascade can be measured by placing probes downstream of the bars. However, the distance between the bars and the leading edges of the cascade is usually small (~25-50% of the chord). Therefore, access is difficult, especially in small scale, high speed cascades. Furthermore, the flow is unsteady. This can result in false readings from conventional instrumentation. Also, due to the presence of the blades, the time-mean inlet stagnation conditions may not be pitchwise uniform in the unsteady flows (Hodson and Dawes, 1996).

An additional problem arises when using a rotating wake generator as in the high speed measurements. The conditions downstream of the moving bars depend on the pitch of the bars and the speed of the bars, amongst others parameters. Therefore, in order to determine the (midspan) inlet conditions, the probes would need to be placed at the same spanwise position as where the exit measurements were performed. This would corrupt the exit measurements.

The above discussion highlights some of the difficulties associated with measuring the time mean conditions at the inlet to the cascade. To avoid these, a calculation procedure is used to determine the (mixed out) conditions downstream of the bars.

A control volume representing the flow through the row of bars, in the relative frame of reference, is shown in figure 3. The drag force, D, represents the force produced by the bars on the fluid. It is taken to act against a direction averaged with both inlet an exit directions. This model is a modified version of the model proposed by Schulte and Hodson (1996). In their model an incompressible analysis of the same control volume is made, assuming that D acts in the same direction as the flow entering in the control volume. The validation of this method for incompressible flow can be found in Schulte (1995). The validation for compressible flow is presented below.

The drag coefficient of the bars, C_d, is defined by

$$C_d = \frac{D}{d(P_{00,rel} - P_{s0})} \qquad (7)$$

and

$$\tan\beta_m = \frac{1}{2}(\tan\beta_0 + \tan\beta_1) \qquad (8)$$

defines the direction against which the drag force acts.

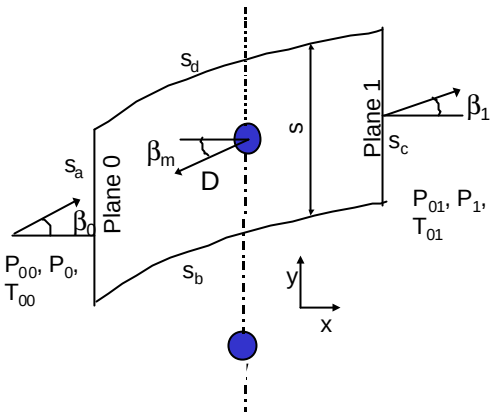

Figure 3. Control volume. Frame of reference fixed to the bars

On surfaces S_b and S_d, periodic boundary conditions apply and no net flow crosses these surfaces. Flow enters the control volume with a uniform velocity through surface S_a and leaves the control volume through surface S_c. It is assumed that mixed out conditions are already reached at surface S_c. The continuity, momentum and energy equations form an implicit system of equations that have to be solved for each inlet condition.

The solution to the system of equations depends on the conditions at plane 0, at plane 1 (through β_1), on the pitch of the bars and on the drag coefficient of the bars, C_d. The value of C_d depends also on the conditions at plane 0. In order to solve the system of equations, the value of C_d has to be known for the range of Reynolds numbers and Mach numbers found in the measurements.

For the determination of C_d, the drag force produced by the bars, D, must be known. To measure D, the wake of one single bar was traversed. Knowing the drag force, the drag coefficient of the bar can be calculated using (7). Figure 4 shows the values of C_d measured for the current experiments.

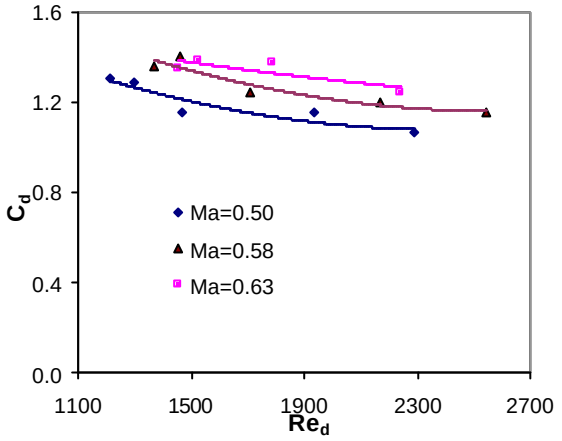

Figure 4. C_d of the bars as a function of the Reynolds number and Mach number relative to the bars.

Knowing the bar relative Reynolds number and Mach number, the value of C_d can be obtained by interpolation using the curve fits of Figure 4. Knowing the value of C_d, the implicit system of equations can be solved for a given value of the conditions upstream the bars and flow angle. Thus, the mixed out conditions downstream the bars can be determined.

The calculation of the conditions downstream of the moving bars will be now validated with experimental results. The measurements were performed in the high speed rotating bar rig. The cascade was removed and a pneumatic probe was placed downstream of the bars. The probe was placed in the plane where the leading edges of the cascade would have been. The conditions upstream the bars corresponded to the design inlet conditions of the cascade.

Downstream of the bars, the probe was traversed in the pitchwise direction at three different spanwise positions. The measured upstream conditions are used to calculate the conditions downstream of the bars by means of the calculation procedure described above. A comparison between the downstream measurements and the calculated values is shown in figure 5. The abscissa represents the radius of the bars at each measurement point. This value is non-dimensionalised by the radius of the bars at 50% of the span and at a pitchwise position that would correspond to the centre of the cascade. The ordinate represents the reduction in stagnation pressure through the row of bars expressed as a fraction of the exit dynamic pressure of the cascade at design conditions. At $r/r_{50\%span}$ equal to 1, the differences between prediction and experiments are less than 0.1% of the cascade exit dynamic pressure. A good agreement between the calculation procedure and the measurements is found, thus validating the method.

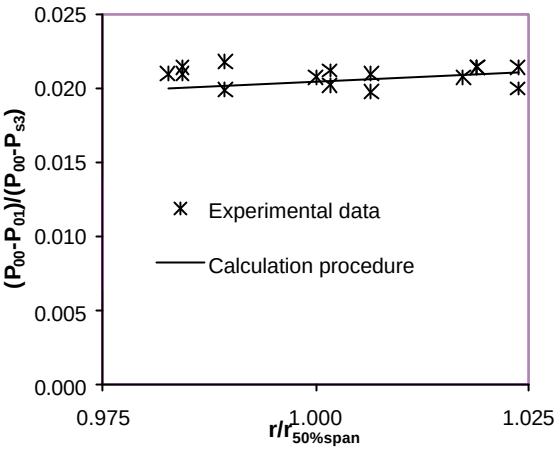

Figure 5. Comparison of experimental data and calculations for the loss of stagnation pressure across the bars at design conditions of the cascade, $Re_3=1.9x10^5$, $Ma_3=0.64$.

Mach number distribution.

Figure 6 shows a plot of the distribution of isentropic Mach number for the high speed and low speed cascades under steady flow consitions. The values are non-dimensionalised by the exit isentropic Mach number. The suction peak occurs at 55% of the suction surface length for both blades. The ratio of the maximum surface isentropic Mach number to the exit isentropic Mach number is about 1.15 for both profiles. The flow separates at about 75% of the suction surface length for both cases. Differences are seen in the region covered by the suction side separation bubble. For a similar length of bubble in both blades, the acceleration due to blockage is bigger in the case of the high speed profile. This is due to compressibility effects. For both profiles, the flow is attached to the blade surface at the trailing edge.

According to Banieghbal et. al, 1995, a pressure side separation bubble occurs in both blades. The Mach number distributions show differences in this region. These could be due to errors in the measurements of the very low velocities associated to the bubble on the low speed profile. The length of the bubble is the same for the high speed and the low speed profile. The bubble extends up to 50% of the pressure surface length. From this position, the flow accelerates towards the exit value.

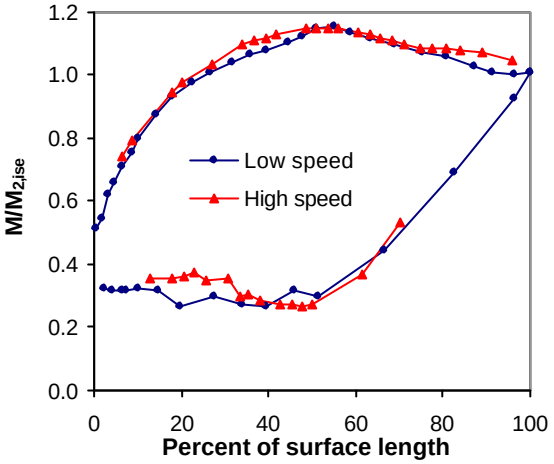

Figure 6. Mach number distribution around the low speed and the high speed profile under steady inflow. Re_3=1.9x10^5

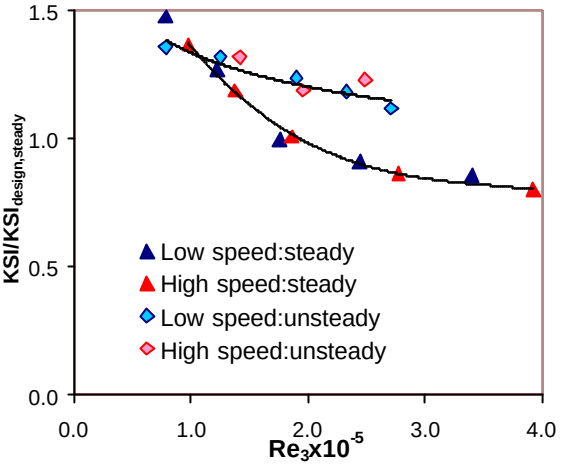

Figure 7. Kinetic Energy (profile) Loss Coefficient KSI versus Reynolds number.

Cascade losses

The LPT blade that both cascades model was designed without considering the effect of unsteady inflow. The blade features a small suction side separation bubble under steady inflow. When wakes are present, wake induced transition always happens near the separation point. The suppression of this small bubble does not produce any benefit. Instead a penalty occurs because more surface is covered by turbulent flow thus increasing the losses.

Pitchwise traverses were performed at midspan behind the high speed and low speed cascade in order to measure the profile loss. Figure 7 shows a plot of the profile losses against Reynolds number for steady and unsteady inflow conditions for both cascades. The design exit Mach number of the high speed blade is 0.64. The kinetic energy loss coefficient KSI is used for the high speed cascade to allow a comparison to be made with the low speed cascade. This is because it is equal to the stagnation pressure loss coefficient when the flow is incompressible. It is seen in the figure that the same trends and the same absolute levels of losses are found for the low speed and high speed cascades. This is true for both steady and unsteady inflow conditions. Figure 7, on its own, answers the question regarding the validity of the low speed approach for the case under consideration.

Hot films results

Up to this point, the comparison between the high speed and the low speed cascade has been made on the bases of profile loss measurements and Mach number distributions. A comparison of the state of the boundary layer along both profiles is also needed. Multi-element hot film anemometers were used to study the development of the blade surface boundary layer. The description of the technique and the description of the presentation of the data can be extensively found in literature (e.g. Banieghbal et. al, 1995).

The anemometers were fitted at the mid-span of the suction surface of the blade in the central passage Figure 8 and figure 9 present distance-time, ST, diagrams of quasi-shear stress from one of the ensembles of the anemometer data, i.e., raw data. Both figures show data obtained at the design conditions. A good agreement is found between the two cases and the same behaviour can be identified. In the results obtained with steady inflow at the design point (not shown here), separation was seen to occur between 75% and 80% of the suction surface. The latter is true for the low speed and the high speed cascade. Figure 8 and figure 9 show that wake induced transition happens near to the point of the steady separation for both high and low speed measurements.

Both sets of the above data were acquired at a logging frequency of 60kHz. The bar passing frequency of the high speed cascade is about 3kHz, which means that approximately 20 points per wake passing are acquired. For the low speed measurements, the bar passing frequency is of the order of 200Hz, implying about 200 points per wake passing. Thus, a better resolution of the wake passing period is obtained in low speed measurements. Furthermore, it was seen before that the values of the lowest turbulent frequencies are of the order of 3kHz for low speed and 100kHz for

high speed. For the current measurements, the low pass filter was set at 30kHz to avoid aliasing of the signal Thus, the lowest turbulent frequencies can be characterized only for the low speed measurements.

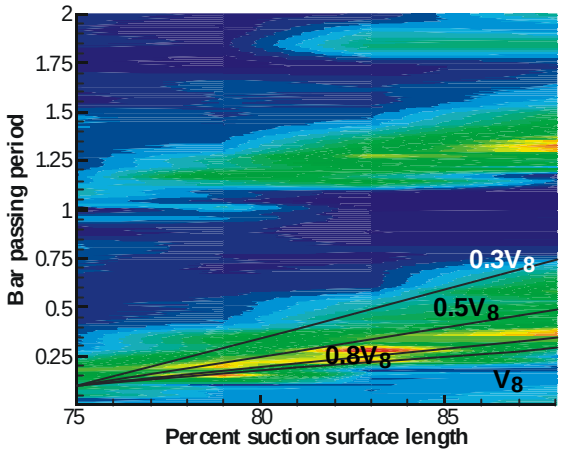

Figure 8. Quasi-shear stress. Design point. High speed cascade , Re_3=1.9x10^5, Ma_3=0.64.

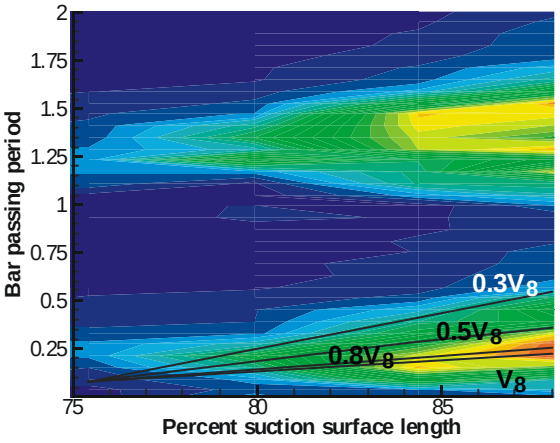

Figure 9. Quasi-shear stress. Design point. Low speed cascade. Re_3=1.9x10^5

CLT2 blade

The above blading is a conventional profile with a lift coefficient of about 0.8 and a turning of about 100 degrees. In order to extent the previous affirmations about the validity of the low speed cascade testing to blades designed with the current techniques, a second case is presented. The CLT2 blade is a profile designed by ITP. It is a high lift, high turning profile designed to take account of unsteady inflow conditions.

The CLT2 blade features a large suction side separation bubble under steady inflow conditions. This bubble is partially or totally suppressed in presence of the wakes coming from an upstream blade row.

Figure 10 presents results of the CLT2 cascade showing the KSI loss coefficient against Mach number. The ordinate is non-dimensionalised using the KSI loss coefficient under steady inflow at design conditions. No dependency with Mach number is found up to an exit Mach number of 0.75, which corresponds to the start of transonic flow. This is the limit of the validity of the low speed approach.

For higher exit Mach numbers, the losses under steady inflow increase and so do the losses under unsteady inflow. Loss reduction due to the wakes is achieved for the entire range of Mach numbers presented.

However, it should be noted that figure 10 is obtained for a given profile. Therefore, the Mach number distribution around the blade becomes more aft loaded when the Mach number is increased.

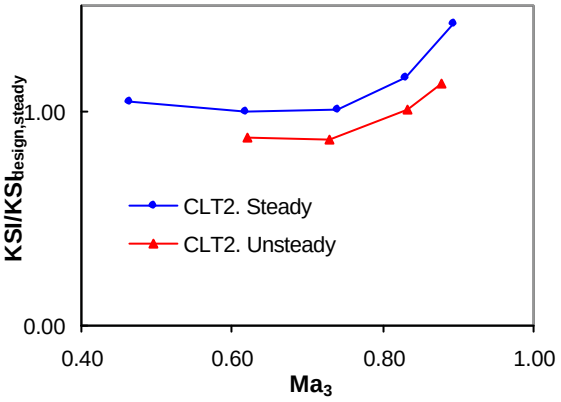

Figure 10. KSI loss coefficient versus Mach number at design Reynolds number (2.0x10^5) for the CLT2 cascade

CONCLUSIONS

The techniques employed in the simulation of unsteadiness in high speed linear cascade testing have been presented and compared to the techniques involved in the low speed tests. Results from a high speed and a low speed cascade, both being models of an existing LPT blade have been compared for steady and unsteady flow conditions.

The results have shown that the same quantitative values of losses are obtained, showing the validity of the low speed approach for profiles with an exit Mach number of the order of 0.64. The previous affirmation has been extended to a high turning, high lift profile designed following current design practices. Measurements of the losses have shown that there is no dependency on Mach number up to the beginning of the transonic range, which is the upper limit of the validity of the low speed approach. A benefit coming from the wakes

is achieved up to an exit Mach number of at least 0.9.

ACKNOWLEDGMENTS

The authors would like to thank T. Chandler for his work on the high speed rotating bar rig. The authors would also like to thank ITP, for the funding of the project and the permission to publish this paper.

REFERENCES

[1] Banieghbal, M.R., Curtis, E.M., Denton, J.D., Hodson, H.P., Huntsman, I., Schulte, V., Harvey, N. W., Steele, A. B., "Wake Passing in LP Turbines Blades," presented at the AGARD conference, Derby, UK, May 8-12, 1995

[2] Boyle, R.J., Simon, F.F., "Mach Number Effects on Turbine Blade Transition Length Prediction" ASME Journal, October 1999, Vol.121.

[3] Brunner, S., Fottner, L., Schiffer, H, "Comparison of Two Highly Loaded Low Pressure Turbine Cascades under the influence of Wake-Induced Transition" ASME 2000-GT-268, 2000

[4] Coton, T., Arts, T., Lefebvre, M., Liamis, N, "Unsteady and calming effects investigation on a very high lift LPT blade", ASME GT-2002-30227, 2002.

[5] Doorly, D.J., "A Study of the effect of wake passing on Turbine Blades", PhD Thesis, Oxford University, 1984.

[6] Halstead, D.E., "Boundary Layer Development in Axial Compressors and Turbines", ASME 95-GT-461, 95-GT-462, 95-GT-463, 95-GT-464, 1995.

[7] Hodson, H.P., "Measurements of Wake-Generated Unsteadiness in the Rotor Passages of Axial Flow Turbines," ASME 84-GT-189, 1984.

[8] Hodson, H.P., Banieghbal, M.R., Dailey, G.M., "The Analysis and Prediction of the Effects of Bladerow Interactions in Axial Flow Turbines", I Mech E conf., Turbomachinery, London, Oct. 7, 1993

[9] Hodson, H.P., Dawes, W.N., "On the Interpretation of Measured Profile Losses in Unsteady Wake-Turbine Blade Interaction Studies", 1996.

[10] Hodson, HP, and Dominy, RG, "Annular Cascade Testing", AGARDograph 328 Advanced Methods for Cascade Testing, AGARD, 1993

[11] Hoerner, S.F. "Fluid Dynamic drag: practical information on aerodynamic drag and hydrodynamic resistance", New Jersey, 1965

[12] Mayle, R. E., "The Role of Laminar-Turbulent Transition in Gas Turbine Engines," ASME 91-GT-261, 1991.

[13] Narashimba, R., "On the distribution of Intermittency in the Transition Region of a Boundary Layer", Journal of Aerospace Sciences, Vol.24, 1957.

[14] Roark, R.J., Young, W.C., "Formulas for Stress and Strain", McGraw-Hill, 1975.

[15] Schlichting, H.,"Boundary Layer Theory", McGraw-Hill, 6th Edition, Translated by Dr J Kestin, McGraw-Hill 1968.

[16] Schulte, V., "Unsteady Separated Boundary Layers in Axial Flow Turbomachinery", PhD Thesis, Cambridge University, 1995.

[17] Schulte, V., Hodson. H.P, "Unsteady Wake-Induced Boundary Layer Transition in High Lift LP Turbines," Journal of Turbomachinery, Vol.120, 1996.

[18] Schulte, V. , Hodson. H.P, "Prediction of the becalmed region for LP turbine profile design," ASME 97-GT-398, 1997.

[19] Schulte, V., Huntsman, I., Hodson. H.P, "Verification of the Controlled Boundary Layer Separation Philosophy for the Design of High Lift, Low Loss Low Pressure Turbines Airfoils", Dec 1992

[20] Wisler, D.C, "Loss Reduction in Axial-Flow Compressors through Low-Speed Model Testing" ASME 84-GT-184, 1984.